Colloid Polym Sci (2011) 289:1839–1846
DOI 10.1007/s00396-011-2501-1

ORIGINAL CONTRIBUTION

Synthesis and characterization of PVA ferrogels obtained through a one-pot freezing–thawing procedure

Jimena S. Gonzalez · Cristina E. Hoppe · Diego Muraca · Francisco H. Sánchez · Vera A. Alvarez

Received: 24 August 2011 / Accepted: 26 August 2011 / Published online: 14 September 2011

Abstract Polyvinyl alcohol (PVA) ferrogels were easily obtained through a one-pot technique that involves co-precipitation of iron salts in the presence of a PVA solution, followed by freezing–thawing cycles of the resulting nanoparticles (NPs) dispersions. The protecting effect of PVA enabled the synthesis of small magnetic NPs that did not agglomerate in the initial solution allowing the synthesis of well-dispersed ferrogels by physical cross-linking. Physical properties of the physically cross-linked ferrogels, as swelling ability, melting temperature, and crystallinity, were barely affected by the presence of NPs, presenting similar or improved values when compared with chemically cross-linked systems. Ferrogels showed super-paramagnetic properties at room temperature that combined with the absence of toxic residues arising from cross-linking agents make them ideal candidates for their use in biomedical applications (artificial muscles, drug delivery, and sensors among others).

Keywords Ferrogel · Iron oxide · Polyvinyl alcohol · Magnetic gel

J. S. Gonzalez · V. A. Alvarez (✉)
CoMP (Composite Materials Group)—Institute of Materials Science and Technology (INTEMA),
University of Mar del Plata and National Research Council (CONICET),
Solís 7575,
7600 Mar del Plata, Argentina
e-mail: alvarezvera@fi.mdp.edu.ar

C. E. Hoppe
Institute of Materials Science and Technology (INTEMA),
University of Mar del Plata and National Research Council (CONICET),
J. B. Justo 4302,
7600 Mar del Plata, Argentina

D. Muraca
Physics Research Institute of Mar del Plata (IFIMAR),
University of Mar del Plata and National Research Council (CONICET),
Dean Funes 3350, 7600 Mar del Plata, Argentina

F. H. Sánchez
Physics Department—Physics Institute of La Plata (IFLP–FCE),
University of La Plata—National Research Council (CONICET),
CC 67,
1900 La Plata, Argentina

Present Address:
D. Muraca
Gleb Wataghin Physics Institute (IFGW),
Universidade Estadual de Campinas,
Rua Sergio Buarque de Holanda, 777 Cidade Universitaria,
Zeferino Vaz Barao Geraldo,
CEP 13083-859 Campinas, São Paulo, Brazil

Introduction

Polymer gels are fascinating materials with multiple and diverse applications as separator agents, solvent absorbers, ion exchangers, diapers, and drug delivery devices between others [1, 2]. They are wet and soft materials constituted by networks of flexible cross-linked chains with a fluid filling their interstitial space [3]. Depending on the type of cross-link forming the network, polymer gels can be classified as chemical gels (cross-linked by covalent bonds) or physical gels (joined by weak forces as hydrogen bonds, van der Waals forces, or hydrophobic and ionic interactions) [1]. Physical gelation is usually a reversible process that occurs through the called sol–gel transition [1].

Large swelling capacities of gels make them attractive not only as absorbents or separators but also as hosts for the development of multifunctional materials. For example, by incorporation of liquid crystals [4] or metal ions [5] to the liquid phase, materials with especial properties have been obtained. In the case of physical gels, the ability to be

reversibly transformed between the liquid and the gelled states adds new advantages to the obtained materials.

Nanocomposite polymeric hydrogels are cross-linked polymer networks swollen with water modified by the presence of nanoparticles (NPs) or nanostructures [6]. NPs can add unique physical properties to the gels as responsiveness to mechanical, optical, thermal, barrier, magnetic or electric stimulation among others [6, 7]. Ferrogels are obtained by incorporation of magnetic NPs to polymeric hydrogels. For their biocompatible nature, iron oxide NPs are the first choice to obtain ferrogels with potential uses in biomedicine [8]. The magnetoelastic properties of such gels give them the potential use as biomembranes [9], biosensors [10], artificial muscles [11], and matrices for drug delivery [12–15]. Size and surface characteristics of NPs, the incorporation approach to the hydrogel, and the procedure used to obtain the polymer network are variables that can strongly influence the final properties of ferrogels [16].

Polyvinyl alcohol (PVA) is a hydrophilic, biocompatible polymer that has been previously used for the synthesis of NPs and nanocomposites in different ways. For example, it has been used as a stabilizing agent in the preparation of ferrofluids based on magnetite obtained by chemical coprecipitation [17]. Noncross-linked films and fibers (by wet spinning) could also be obtained from this polymer and magnetic NPs obtained by in situ precipitation within the matrix [18].

PVA is an interesting polymer for the synthesis of biocompatible high-strength hydrogels [19]. This polymer can be covalently cross-linked through the use of chemical agents [20], electron beam, or γ-irradiation [21]. The use of cross-linking agents as glutaraldehyde (GA) presents disadvantages associated with the presence of residual amounts of toxic molecules in the gel, undesirable for biomedical applications [22]. Use of complex irradiation techniques, as electron beam or γ-irradiation, although does not leave behind toxic impurities, has usually problems associated with bubbles formation [23]. A third mechanism of hydrogel preparation involves physical cross-linking by freezing–thawing. This is a thermal strategy not only restricted to the formation of cross-linking points in polymers but also applied to many different processes. It has been used, for example, to fabricate stable nanorods with rigid walls as a simple postsynthesis temperature program [24]. In the formation of hydrogels, crystallites formed during freezing–thawing cycles act as the cross-linking points of the matrix [25, 26]. Such materials exhibit higher mechanical strength than gels obtained by chemical or irradiative techniques and only require the use of repeated and easy freezing and thawing cycles [25, 27].

PVA and iron oxide NPs have been previously used to obtain ferrogels [18, 28–30]. Most of these approaches are based in a first step involving the synthesis of magnetic NPs followed by their incorporation in a PVA solution that will be subsequently cross-linked to give a ferrogel [31]. The main problem associated with this technique is the almost unavoidable formation of NPs aggregates [32]. This problem is usually minimized by using chemically compatible coatings to functionalize the NPs. However, these procedures usually add complexity and extra time to the ferrogel synthetic process. The synthesis of NPs in the presence of a PVA solution, previous to the formation of the gel, could avoid these problems. After the synthesis, the obtained ferrofluids can be used to obtain ferrogels by chemical cross-linking strategies. However, most of the chemical cross-linking agents are toxic, which decrease the potentiality of the systems in biomedical applications as a consequence of the unavoidable presence of residues.

In this work, an in situ technique for the synthesis of NPs in presence of PVA was combined with a freezing–thawing (FT) procedure for the one-pot generation of ferrogels. Freezing–thawing is a nontoxic, easy way to obtain PVA gels with good properties. Magnetic, thermal, and swelling properties were analyzed and compared with chemically cross-linked ferrogels in order to evaluate the potential applications of these systems in biomedicine.

Experimental methods

Materials

PVA was purchased from Aldrich with a hydrolysis degree higher than 98–99% and a molecular average weight of 93,000 g/mol. Iron(II) sulfate heptahydrated and iron(III) chloride hexahydrated were from Cicarelli laboratory (Argentina); glutaraldehyde was from QRS analytical (Argentina); hydrochloric acid and methanol were from Biopack (Argentina); acetic acid buffer, sulfuric acid, and ammonium hydroxide were from Anedra laboratory (Argentina).

Synthesis of gels

Twenty grams of PVA was dissolved in 200 ml of a solution containing 2.97 g $Cl_3Fe{\cdot}6H_2O$, 1.485 g of $SO_4Fe{\cdot}7H_2O$ and 1 ml of HCl (to avoid oxidation of Fe(II)) at 85 °C under slow magnetic stirring during 4 h. After cooling to room temperature, 10 ml of NH_3 was added to the clear solution to produce the basic coprecipitation (pH=10) of magnetite NPs (Fe_3O_4). Reaction is showed in Eq. 1.

$$Fe^{+2} + 2Fe^{+3} + 8\ OH^- \rightarrow Fe_3O_4 + 4H_2O \quad (1)$$

To obtain thin samples of the ferrogels, cross-linking was carried out on flat moulds using 10 ml aliquots of the initial solution. For samples obtained by freezing–thawing (FT ferrogels), the solution was frozen for 1 h to −18 °C and then placed at 25 °C (thawing process) for the same time in order to produce cross-linkings. This procedure of freezing–thawing was performed three times. The obtained film was dried until constant weight (35 °C, 24 h). This is the optimal number of cycles for the formation of a stable three-dimensional network with good mechanical properties [33].

To obtain ferrogels chemically cross-linked by glutaraldehyde (GA ferrogels), a cross-linking solution obtained by mixing methanol (3 ml, 50 vol.%), acetic acid (2 ml, 10 vol. %), and glutaraldehyde (1 ml, 5 vol.%) was prepared. Of this solution 2.8 ml was added on 10 ml of the initial PVA solution and then cast onto an antiadherent container. Drying was carried out in an oven at 35 °C for 24 h (until constant weight). A similar procedure in the absence of iron salts was used to obtain FT and GA hydrogels devoid of NPs used for comparative purposes.

Techniques

DSC measurements were carried out in a Shimadzu DSC-50. Samples were scanned from room temperature to 250 °C at a heating rate of 10 °C/min, under nitrogen atmosphere. The melting temperature (T_m) was taken from the obtained curve at the peak value. The crystallinity degree (X_{cr}) was calculated from the following equation:

$$X_{cr}\% = \frac{\Delta H}{w_m \Delta H_c} \times 100 \quad (2)$$

where ΔH was determined by integrating the area under the melting peak over the range 190–240 °C, ΔH_c was the heat required for melting a 100% crystalline PVA sample (138.6 J/g) [34, 35], and w_m was the weight fraction of PVA (obtained from TGA curves).

Ferrogel morphologies were observed by FESEM in a Zeiss ULTRA plus instrument. The samples were lyophilized and fractured in liquid air before testing.

Thermogravimetric studies were performed in a Shimadzu TGA-DTGA 50. All dried samples (35 °C, 24 h) were analyzed from room temperature to 900 °C at 10 °C/min under air atmosphere. Degradation temperature (T_p) and nanoparticles content (percentage of NPs) were obtained from these measurements. X-ray diffraction (XRD) analysis was carried out using an analytical expert instrument (K_∞Cu=1.54 Å) from 2θ=3° to 60° at a rate of 2°/min.

Swelling determinations were carried out in distilled water at 25 °C. All samples were dried before immersion for 24 h at 35 °C. The swelling degree (M_t) percentage was determined by the following equation:

$$M_t\% = \frac{M_f - M_i}{w_m M_i} \times 100 \quad (3)$$

were M_i and M_f are the mass of the sample before and after immersion respectively and w_m was the weight fraction of PVA (obtained from TGA curves).

To perform gel fraction measurements, slices of the samples were placed in a fan oven at 35 °C until no change in mass was observed. After this first drying process, they were immersed in distilled water for 4 days to rinse away soluble species. Subsequently, the immersed sample was removed from distilled water and dried at 35 °C until constant weight was reached. Therefore the gel fraction (GF) can be calculated as follows:

$$\mathrm{GF}\% = \frac{W_f - W_{NPs}}{W_i - W_{NPS}} \times 100 \quad (4)$$

where W_i and W_f are the mass of the dried gels before and after immersion in water respectively and W_{NPs} is the mass of NPs obtained from TGA curves.

Magnetic properties of the samples were investigated by SQUID magnetometry. Magnetization of FT and GA ferrogel samples was measured at room temperature (25 °C) as a function of the applied magnetic field between −20 to 20 kOe.

Results and discussions

GA and FT ferrogels were obtained by direct cross-linking of PVA/magnetite dispersions. This procedure involves a first coprecipitation step, in which PVA protecting ability is used to control the size and aggregation level of NPs, and a second cross-linking step of the stable resulting aqueous dispersions. Adsorption of PVA on NP surface is expected to occur during the first step. This adsorption process has strong influence on size, shape, aggregation level and magnetization of NPs, and, consequently, on final properties of the ferrogels [36]. On the other hand, the strong interactions between NPs and PVA polymer chains could affect the efficiency of freezing–thawing procedure and the final properties of PVA gels. Hence, a detailed analysis of the synthesis procedure and final magnetic and thermal properties of these materials is highly desirable in order to evaluate their potential performance as smart materials.

The first interesting aspect of the synthesis is the high stability and optical homogeneity of the initial NPs–PVA dispersions. Presence of OH groups on the PVA backbone gives to this polymer high affinity by oxide surfaces. Hence, adsorption of polymer chains controls growth and aggregation and avoids formation of big flocculates and

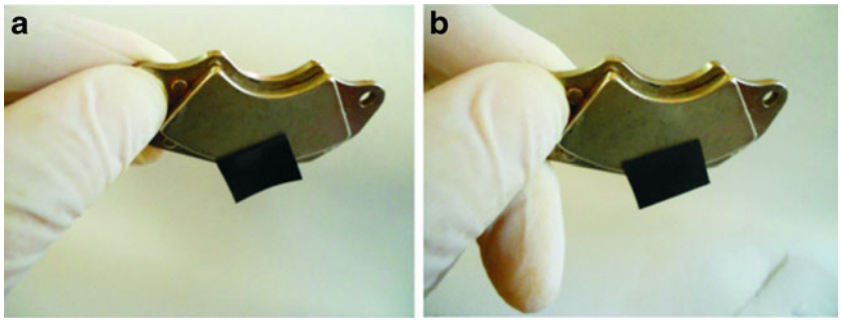

Fig. 1 Photographs of FT- (**a**) and GA- (**b**) obtained ferrogels

clusters of NPs. Thanks to this high dispersion stability, cross-linking can be carried out directly on the prepared NPs dispersion without previous separation, stabilization, or purification steps. In this case, films were obtained by casting an aliquot of the solution on antiadherent flat moulds. To obtain FT ferrogels, successive freezing (in a commercial freezer) and thawing (at room temperature) steps were applied on the samples. Drying was performed at 35 °C after 3 FT cycles [33]. For comparative purposes similar samples were chemically cross-linked with glutaraldehyde. With this cross-linker, acetal bridges form between the pendant hydroxyl groups of the PVA chains giving place to a network. It is necessary to keep in mind that, as with any other cross-linker agent, residual amounts of reagents always remained in the gel that only can be removed after time-consuming extraction procedures. The presence of toxic residues arising from chemical cross-linking processes (GA, methanol, acetic acid, etc.) is unacceptable for pharmaceutical and biomedical applications [35].

Figure 1 shows photographs of the obtained ferrogels and their behavior when exposed to the field of a permanent magnet. This simple analysis showed the presence of a magnetic phase contained in the PVA matrix.

The presence of a homogeneous dispersion of small particles in both kinds of samples was confirmed by FESEM performed on cryofractured samples (Figs. 2 and 3). NPs size was below 50 nm for in both ferrogels with only low levels of aggregation detected. These results confirm the efficiency of PVA in the protection against growth and aggregation of magnetite NPs generated by coprecipitation in aqueous solution. On the other hand, it shows that the FT procedure is useful for the synthesis of well-dispersed ferrogels with similar characteristics to that obtained by chemical cross-linking.

XRD measurements performed on both, FT and GA films (devoid of NPs), are shown in Fig. 4. Main characteristic diffraction peaks of semicrystalline PVA located at 19.8° and 22.9° (2θ) which correspond to the (1 0 1) and (1 0 $\bar{1}$) reflection planes, respectively, are present in both diffractograms [37, 38]. In the case of ferrogels, an additional peak centered at 35.5° (2θ) was observed. This peak agrees with the (3 1 1) plane reflection, the most intense diffraction peak for magnetite or maghemite (19-0629 JCPDS, Joint Committee on Powder Diffraction Standards) and confirms the presence of this oxide in the PVA matrix. NPs crystal size in FT ferrogels was also evaluated using Scherrer equation and XRD data [39]. The average crystal size was estimated to be 9–10 nm.

Final concentration of NPs in the polymeric matrix was determined by thermogravimetric analysis. Based on the initial formulation, theoretical magnetite content should be 6 wt.% in anhydrous samples expressed in terms of completely oxidized γ-Fe_2O_3. After subtraction of the amount of carbonaceous residues arising from incomplete degradation of PVA (1 wt.%) and bound water, NPs content was determined to be near identical to the calculated value for both samples, indicating absence of exudation of NPs during drying.

To address the effect of NPs on the final properties of the gels, thermal and swelling experiments were carried out on hydro- and ferrogels samples obtained by FT. Table 1 shows

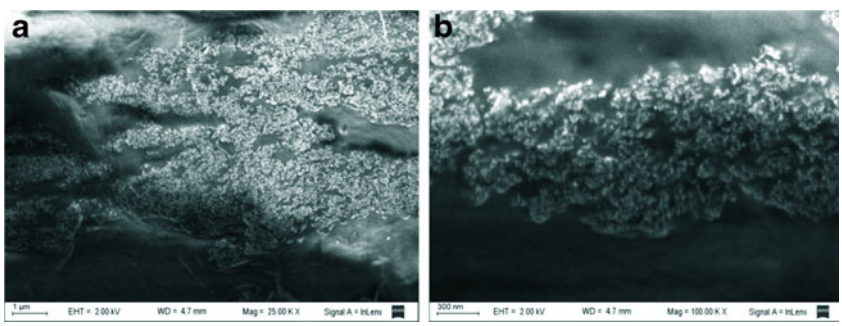

Fig. 2 **a** FESEM image of an FT ferrogel sample containing 6 wt.% of magnetite. **b** Magnification of a region in **a**

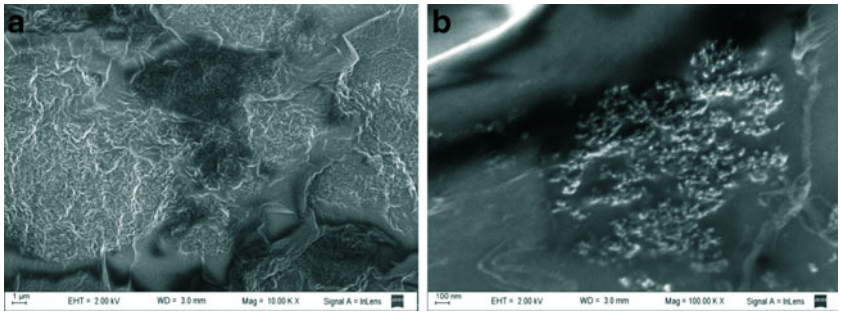

Fig. 3 **a** FESEM images of a GA ferrogel sample containing a 6 wt.% of magnetite. **b** Magnification of a region in **a**

the X_{cr} and T_m values for FT samples as determined by DSC (Fig. 5). Both crystallinity degree and melting temperature show a slight decrease with the presence of NPs, indicating the formation of a lower amount of crystallites of smaller size when compared with the neat matrix. This is also supported by the decrease in T_p observed for FT samples with 6 wt.% of NPs. A matrix formed by smaller crystallites would be easier to degrade than one formed by bigger crystals. Hence, thermal behavior seems to indicate that presence of NPs precludes the ability of PVA chains to order into a crystalline structure [12] which is translated in a lower crystallinity and a decrease in crystallite size.

Gravimetric water uptake was measured to determine swelling ability of the samples. This is the most commonly used method to evaluate the effect of cross-linking on water transport in PVA [40]. Results for FT and GA samples are showed in Fig. 6. As can be observed, GA samples (neat matrix and ferrogel) showed a constant swelling behavior, indicating that NPs have a low influence on the network properties. In this case, swelling was mainly determined by the type and amount of cross-linking agent, the same for both samples.

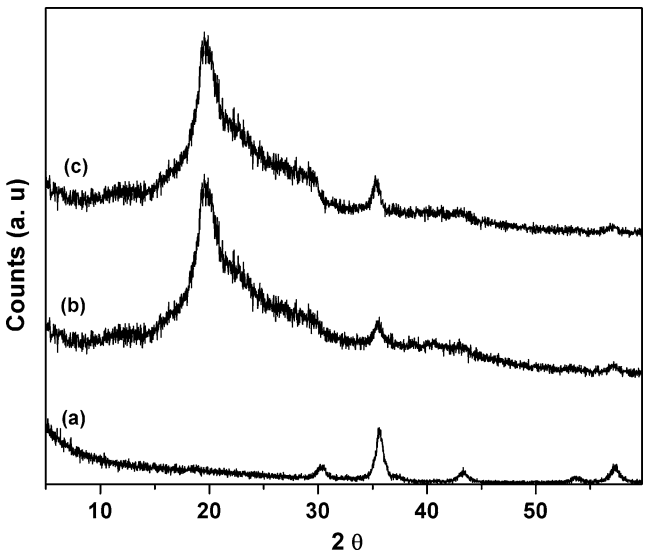

Fig. 4 XRD curves for magnetite (*a*), FT ferrogel (*b*), and GA ferrogel samples (*c*)

A completely different behavior was observed for the FT samples. In this case, the presence of NPs strongly decreased the swelling capacity of the gel and increased its dimensional stability. This effect could be understood analyzing the mechanism behind cross-linking in FT physical gels. In these hydrogels, cross-linking points are small crystallites that join more than three PVA chains. Size and amount of these crystallites depend on the number of FT cycles to which samples are submitted, as well as composition, molecular weight, and concentration of the initial solution [33, 37, 38]. It seems possible that the presence of NPs can increase the total number of crystallites formed (i.e., the number of cross-linking points) reducing the swelling ability of the matrix. On the other hand, interaction of the PVA chains with NPs might conduct to the formation of low-mobility regions that can act as additional physical cross-linking points, as reported for formation of Fe_3O_4 NPs in the presence of κ-carrageenan. In this reported work, NPs promote gelation and increase strength of gels, as viewed by the increase of the viscoelastic moduli and gelation temperatures [6, 41].

In summary, the presence of NPs influenced the efficiency of PVA to crystallize which was evidenced by a decrease in the global crystallinity and the size of the crystalline zones. However, swelling decreased with the presence of NPs pointing to an increase of the cross-linking density. Explanation of both facts could be found in the formation of a high amount of small crystallites as a consequence of the presence of NPs acting as nucleation centers and/or to the creation of low-mobility regions that can act as additional cross-linking points (Table 1). As can be observed, the percentage of GF value increases with the presence of NPs, indicating that a higher number of PVA chains was incorporated to the network.

Table 1 Main characteristics of FT ferro- and hydrogels

Sample	X_{cr} %	T_m (°C)	GF %
Hydrogel FT	31.8	220.5	67.30±3.55
Ferrogel FT	26.2	215.0	84.17±0.66

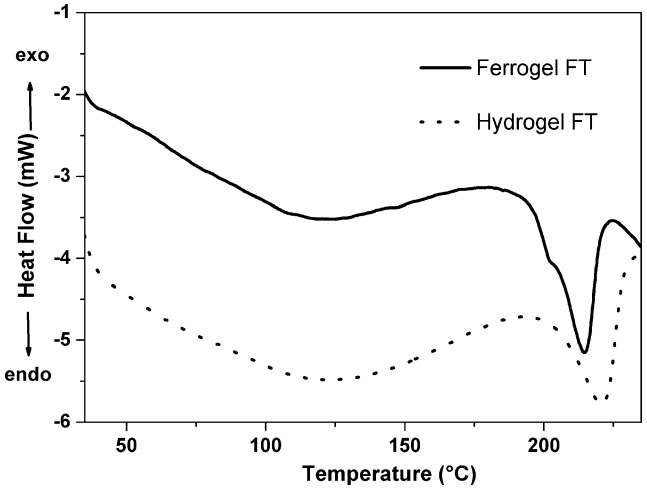

Fig. 5 DSC traces obtained at 10 °C/min under N2 flow, for the FT hydrogel (*dotted line*) and the FT ferrogel (*solid line*) containing 6 wt.% of Fe_3O_4

Magnetic properties

As observed in Fig. 7a, the magnetic response of the GA sample was lesser than the FT sample. Both of them present almost complete superparamagnetic behavior at room temperature, with very low values of coercivity (10 Oe in both cases, Fig. 7b). This low coercivity can be attributed to a small fraction of particles either sufficiently large as to be blocked at room temperature or experiencing nonnegligible interactions among them due to NPs concentration fluctuations or even to some degree of NPs agglomeration.

Considering the amount of magnetic particles in the gels (6 wt.%) and the obtained saturation magnetization values of 3.64 and 3.39 emu/g for the FT and GA samples, respectively, saturation magnetization of NPs can be calculated as 60.59 and 56.43 emu/g.

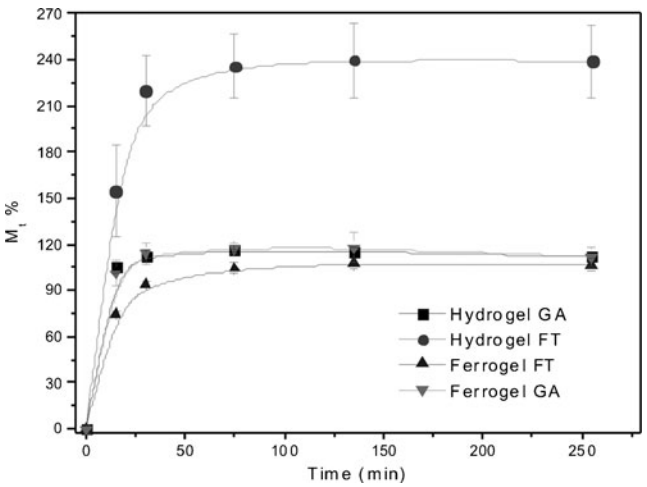

Fig. 6 Gravimetric water uptake as a function of time for GA and FT hydro-and ferrogel samples

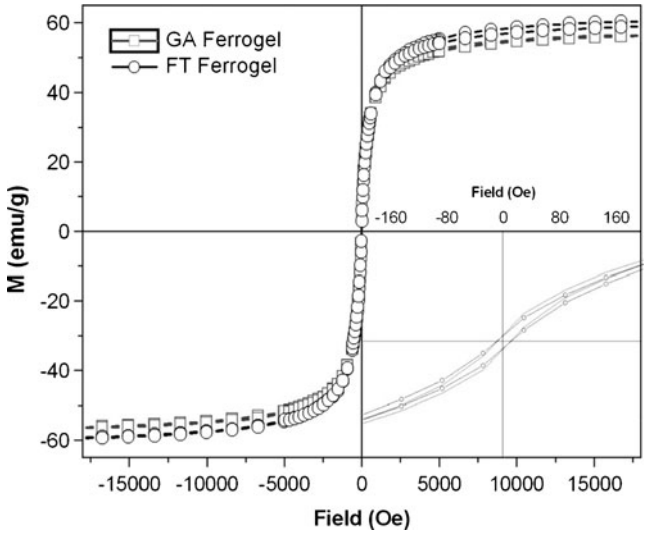

Fig. 7 **a** Magnetization-applied field curves of two samples at room temperature. **b** The *inset* shows a low field detail of the curves

Typically, NPs magnetization decreases as its size diminishes. In a recent work, Laurent et al. [42] have shown that saturation magnetization of iron oxide NPs with average sizes of 4.48 and 5.59 nm were 20 and 58 emu/g, respectively. Wu et al. [43] have reported values of magnetization between 16.80 and 24.10 emu/g for magnetite NPs with sizes below 5 nm; Vargas et al. [44] have obtained values of saturation magnetization near to 20 emu/g for 5-nm magnetite particles, and Majewski and Thierry [45] have reported saturation magnetization between 55 and 65 emu/g for 20 nm magnetite NPs. Hence the saturation magnetization results obtained for GA and FT samples are well consistent with the values

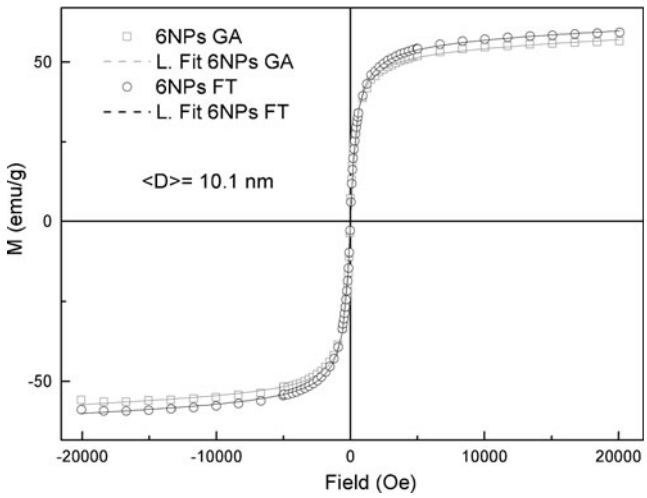

Fig. 8 *Circles and squares* experimental data of the H decreasing branches of curves of Fig. 7 for the GA and FT samples. *Lines* fits assuming a hyperbolic distribution of NP magnetic moments and a Langevin response for each single moment. A shift in the horizontal axis was allowed to account for coercivity effects

previously reported by others authors for nanoparticles between 10 and 20 nm.

To corroborate the previous results, a Langevin (L) distributed function (Fig. 8) was used to fit the experimental data (continuous line):

$$M = \frac{N\langle\mu\rangle \int_0^\infty \mu L(\alpha\mu)P(\mu)d\mu}{\int_0^\infty \mu P(\mu)d\mu} \quad (5)$$

were $\alpha=B/kT$, B is the magnetic field, k is the Boltzman constant, and T is the temperature; N is the number of particles per unit mass, μ is particle magnetic moment, $P(\mu)$ the magnetic moments distribution, and $<\mu>$ moment mean value defined as:

$$\langle\mu\rangle = \frac{\int_0^\infty \mu P(\mu)d\mu}{\int_0^\infty P(\mu)d\mu} \quad (6)$$

The mean size of the NPs was estimated to be 10.1 nm for both the FT and GA samples, confirming previous obtained results.

Conclusions

Superparamagnetic ferrogels were obtained by a one-pot procedure based on the freezing–thawing of ferrofluids obtained by in situ synthesis of iron oxide in the presence of PVA. A good dispersion of NPs in the PVA matrix, with typical sizes around 10 nm, could be obtained thanks to the stabilization properties of PVA that avoid initial aggregation of crystals during coprecipitation. The physical cross-linking approach allowed the synthesis of materials free of toxic residues, which results to its paramount importance regarding their potential biomedical applications. Saturation magnetization of NPs embedded in the gels was smaller than the bulk value but within the range expected for 10 nm NPs and similar to that obtained for GA cross-linked materials. This indicated that NPs were completely retained in the gel (no exudation occurred) and that magnetic properties could be efficiently transferred to the nanocomposites in a procedure that increased, at the same time, gel dimensional stability and cross-linking density. All these advantages make these materials very promising for their application in biomedical fields.

Acknowledgments This study was supported by National Scientific and Technical Research Council (CONICET), National Agency of Scientific and Technology Promotion (ANPCyT), and National University of Mar del Plata (UNMdP). The authors would like to thank the cooperation support by of Eng. David D' Amico in the XRD analyses.

References

1. Osada Y, Gong JP, Tanaka YJ (2004) Polymer gels 1. J Macromol Sci Polymer Rev C44:87–112. doi:10.1081/MC-120027935
2. Sonmez HB, Wudl F (2005) Cross-linked poly(orthocarbonate)s as organic solvent sorbents. Macromolecules 38:1623–1626. doi:10.1021/ma048731x
3. Jilie K, Li M (2008) Smart polymers. Applications in biotechnology and biomedicine. In: Galaev I, Mattiasson B (eds) Smart hydrogels. CRC Press, Boca Raton. ISBN 13:978-0-8493-9161-3
4. Kato T, Hirai Y, Nakaso S, Moriyama M (2007) Liquid-crystalline physical gels. Chem Soc Rev 36:1857–1867
5. Feldgitscher C, Peterlik H, Puchberger M, Kickelbick G (2009) Structural investigations on hybrid polymers suitable as a nanoparticle precipitation environment. Chem Mater 21:695–705. doi:10.1021/cm802171s
6. Schexnailder P, Schmidt G (2009) Nanocomposite polymer hydrogels. Colloid Polym Sci 287:1–11. doi:10.1007/s00396-008-1949-0
7. Filipcsei G, Csetneki I, Szilágyi A, Zrínyi M (2007) Magnetic field-responsive smart polymer composites. Adv Polym Sci 206:137–189
8. Schewertmann U, Cornell RM (1991) Iron oxides in the laboratory: preparation and characterization. VCH, Weinheim
9. Samba Sivudu K, Rhee KY (2009) Preparation and characterization of pH-responsive hydrogel magnetite nanocomposite. Colloid Surface Physicochem Eng Aspect 349:29–34. doi:10.1016/j.colsurfa.2009.07.048
10. Liu Z, Liu Y, Yang H, Yang Y, Shen G, Yu R (2005) A phenol biosensor based on immobilizing tyrosinase to modified core-shell magnetic nanoparticles supported at a carbon paste electrode. Anal Chim Acta 533(1):3–9. doi:10.1016/j.aca.2004.10.077
11. Mao L, Hu Y, Piao Y, Chen X, Xian W, Piao D (2005) Structure and character of artificial muscle model constructed from fibrous hydrogel. Curr Appl Phys 5(5):426–428. doi:10.1016/j.cap.2004.11.003
12. Paradossi G, Cavalieri F, Chiessi E, Spagnoli C, Cowman MK (2003) Poly(vinyl alcohol) as versatile biomaterial for potential biomedical applications. J Mater Sci Mater Med 14:687. doi:10.1023/A:1024907615244
13. Matejka L, Dukh O, Meissner B, Hlavatá D, Brus J, Strachota A (2003) Block copolymer organic–inorganic networks. Formation and structure ordering. Macromolecules 36:7977–7985. doi:10.1021/ma034234p
14. Hu SH, Liu TY, Liu DM, Chen SY (2007) Controlled pulsatile drug release from a ferrogel by a high-frequency magnetic field. Macromolecules 40(19):6786–6788. doi:10.1021/ma0707584
15. Satarkar N, Zach Hilt J (2008) Magnetic hydrogel nanocomposites for remote controlled pulsatile drug release. J Control Release 130:246–251. doi:10.1016/j.jconrel.2008.06
16. Liu TY, Hu SH, Liu TY, Liu DM, Chen SY (2006) Magnetic-sensitive behavior of intelligent ferrogels for controlled release of drug. Langmuir 22(14):5974–5978. doi:10.1021/la060371e
17. Qiu X-P, Winnik F (2000) Preparation and characterization of PVA coated magnetic nanoparticles. Chin J Polym Sci 18 (6):535–539
18. Lin H, Watanabe Y, Kimura M, Hanabusa K, Shirai H (2003) Preparation of magnetic poly(vinyl alcohol) (PVA) materials by in situ synthesis of magnetite in a PVA matrix. J Appl Polym Sci 87 (8):1239–1247. doi:10.1002/app.11520
19. Vacile C, Kulshshreshta AK (2003) Handbook of polymer blends and composites, vol 4. Rapra Technology Ltd., Shrewsbury
20. Matsuyama H, Teramoto M, Urano H (1997) Analysis of solute diffusion in poly(vinyl alcohol) hydrogel membrane. J Membr Sci 126:151–160. doi:10.1016/S0376-7388(96)00287-6

21. Hill DJT, Whittaker AK et al (2011) Water diffusion into radiation crosslinked PVA–PVP network hydrogels. Radiat Phys Chem 80:213–218. doi:10.1016/j.radphyschem.2010.07.035
22. Peppas NA, Mongia NK (1997) Ultrapure poly(vinyl alcohol) hydrogels with mucoadhesive drug delivery characteristics. Eur J Pharm Biopharm 43:51–58
23. Griffith Cima L, Lopina ST (1995) Network structures of radiation-cross-linked star polymer gels. Macromolecules 28:6787–6794. doi:10.1021/ma00124a013
24. Mahmoudi M, Simchi A, Imani M, Stroeve P, Sohrabi A (2010) Templated growth of superparamagnetic iron oxide nanoparticles by temperature programming in the presence of poly(vinyl alcohol). Thin Solid Films 518:4281–4289
25. Hassan CM, Peppas NA (2000) Structure and applications of poly (vinyl alcohol) hydrogels produced by conventional crosslinking or by freezing/thawing methods. Adv Polym Sci 153:37–65
26. Willcox PJ, Howie DW Jr, Schmidt-Rohr K, Hoagland DA, Gido SP, Pudjianto S et al (1999) Microstructure of poly(vinyl alcohol) hydrogels produced by freeze/thaw cycling. J Polymer Sci B Polymer Phys 37:3438–3454. doi:10.1002/(SICI)1099-0488(19991215)37:2
27. Yang X, Liu Q, Chen X, Zhu Z (2008) Investigation on the formation mechanisms of hydrogels made by combination of γ-ray irradiation and freeze–thawing. J Appl Polym Sci 108:1365. doi:10.1002/app.27832
28. López D, Cendoya I, Torres F, Tejada J, Mijangos C (2001) Preparation and characterization of poly(vinyl alcohol) based magnetic nanocomposites. 1. Thermal and mechanical properties. J Appl Polym Sci 82:3215–3222. doi:10.1002/app.2180
29. Szabó D, Czakó-Nagy I, Zrínyi M, Vértes AJ (2000) Magnetic and Mössbauer studies of magnetite-loaded polyvinyl alcohol hydrogels. J Colloid Interface Sci 221:166–172. doi:10.1006/jcis.1999.6572
30. Bertoglio P, Jacobo SE, Daraio ME (2010) Preparation and characterization of PVA films with magnetic nanoparticles: the effect of particle loading on drug release behavior. J Appl Polym Sci 115:1859–1865. doi:10.1002/app.31315
31. Resendiz-Hernandez PJ, Rodriguez-Fernandez OS, Garcia-Cerda LA (2008) Synthesis of poly(vinyl alcohol) magnetite ferrogel obtained by freezing thawing technique. J Magn Magn Mater 320: e373–e376. doi:10.1016/j.jmmm.2008.02.073
32. Theppaleak T, Tumcharern G, Wichai U, Rutnakornpituk M (2009) Synthesis of water dispersible magnetite nanoparticles in the presence of hydrophilic polymers. Polym Bull 63:79–90. doi:10.1007/s00289-009-0075-6
33. Gonzalez JS, Alvarez VA (2011) In: Wythers MC (ed) Advances in materials science research, vol 10. Nova, Commack, pp 265–285. ISBN 978-1-61324-511-8
34. Mallapragada SK, Peppas NA (1996) Mechanism of dissolution of semicrystalline poly(vinyl alcohol) in water. J Polymer Sci B Polymer Phys 34:1339–1346
35. Peppas NA, Merrill EW (1976) Differential scanning calorimetry of crystallized PVA hydrogels. J Appl Polym Sci 20:1457–1465
36. Albornoz C, Sileo EE, Jacobo SE (2004) Magnetic polymers of maghemite (γ-Fe2O3) and polyvinyl alcohol. Phys B Condens Matter 354(31):149–153. doi:10.1016/j.physb.2004.09.038
37. Ricciardi R, Auriemma F, Gaillet C, De Rosa C, Laupretre F (2004) Investigation of the crystallinity of freeze/thaw poly(vinyl) alcohol hydrogels by different techniques. Macromolecules 37:9510–9516. doi:10.1021/ma048418v
38. Gupta S, Pramanik AK, Kailath A, Mishra T, Guha A, Nayar S, Sinha A (2009) Composition dependent structural modulations in transparent poly(vinyl alcohol) hydrogels. Colloid Surf B Biointerfaces 74:186–190. doi:10.1016/j.colsurfb.2009.07.015
39. Cullity BD (1978) Elements of X-ray diffraction, 2nd edn. Addison-Wesley, Reading
40. Kokabi M, Sirousazar M, Hassan ZM (2007) PVA–clay nanocomposite hydrogel for wound dressing. Eur Polym J J43:773–781. doi:10.1016/j.eurpolymj.2006.11.030
41. Daniel-da-Silva AL, Lóio R, Lopes-da-Silva JA, Trindade T, Goodfellow BJ, Gil AM (2008) Effects of magnetite nanoparticles on the thermorheological properties of carrageenan hydrogels. J Colloid Interface Sci 324:205–211. doi:10.1016/j.jcis.2008.04.051
42. Laurent S, Forge D, Port M, Roch A, Robic C, Vander Elst L, Muller RN (2008) Magnetic iron oxide nanoparticles: synthesis, stabilization, vectorization, physicochemical characterizations, and biological applications. Chem Rev 108:2064–2110. doi:10.1021/cr068445e
43. Wu JH, Ko SP, Liu HL, Kim S, Ju JS, Kim YK (2007) Sub 5 nm magnetite nanoparticles: synthesis, microstructure, and magnetic properties. Mater Lett 61:3124–3129. doi:10.1016/j.matlet.2006.11.032
44. Vargas JM, Lima E Jr, Zysler RD, Duque JGS, De Biasi E, Knobel M (2008) Effective anisotropy field variation of magnetite nanoparticles with size reduction. Eur Phys J B 64:211–218. doi:10.1140/epjb/e2008-00294-6
45. Majewski P, Thierry B (2007) Functionalized magnetite nanoparticles—synthesis, properties, and bio-applications. Crit Rev Solid Mater Sci 32:203–215. doi:10.1080/10408430701776680